INL/CON-10-18014
PREPRINT

Thermo-Mechanical Analysis of Coated Particle Fuel Experiencing a Fast Control Rod Ejection Transient

HTR 2010

Javier Ortensi
Brian Boer
Abderrafi M. Ougouag

October 2010

The INL is a
U.S. Department of Energy
National Laboratory
operated by
Battelle Energy Alliance

Proceedings of HTR 2010
Prague, Czech Republic, October 18-20, 2010
Paper 100

Thermo-Mechanical Analysis of Coated Particle Fuel Experiencing a Fast Control Rod Ejection Transient

Javier Ortensi, Brian Boer, Abderrafi M. Ougouag
Idaho National Laboratory
P.O. Box 1625, Idaho Falls, Idaho 83415, USA
phone: +1-208-5264256, javier.ortensi@inl.gov

Abstract – *A rapid increase of the temperature and the mechanical stress is expected in TRISO coated particle fuel that experiences a fast Total Control Rod Ejection (TCRE) transient event. During this event the reactor power in the pebble bed core increases significantly for a short time interval. The power is deposited instantly and locally in the fuel kernel. This could result in a rapid increase of the pressure in the buffer layer of the coated fuel particle and, consequently, in an increase of the coating stresses. These stresses determine the mechanical failure probability of the coatings, which serve as the containment of radioactive fission products in the Pebble Bed Reactor (PBR). A new calculation procedure has been implemented at the Idaho National Laboratory (INL), which analyzes the transient fuel performance behavior of TRISO fuel particles in PBRs. This early capability can easily be extended to prismatic designs, given the availability of neutronic and thermal-fluid solvers. The full-core coupled neutronic and thermal-fluid analysis has been modeled with CYNOD-THERMIX. The temperature fields for the fuel kernel and the particle coatings, as well as the gas pressures in the buffer layer, are calculated with the THETRIS module explicitly during the transient calculation. Results from this module are part of the feedback loop within the neutronic-thermal fluid iterations performed for each time step. The temperature and internal pressure values for each pebble type in each region of the core are then input to the PArticle STress Analysis (PASTA) code, which determines the particle coating stresses and the fraction of failed particles. This paper presents an investigation of a Total Control Rod Ejection (TCRE) incident in the 400 MWth Pebble Bed Modular reactor design using the above described calculation procedure. The transient corresponds to a large reactivity insertion reaching 41 times the nominal power in 0.5 seconds. For each position in the core the coated particle temperature and the stress history during a TCRE transient has been computed and the fuel failure probability has been quantified.*

I. INTRODUCTION

Traditionally thermo-mechanical analysis of coated particle fuel is conducted in fuel performance codes. Power and bulk temperature information are used in the fuel performance code to conduct detailed thermo-mechanical calculations. These calculations produce expected failure fractions for the conditions that are input to the code, which normally originate from a transient calculation.

The novel capability included in this work focuses on generating a predictive capability in a whole core model. This approach allows the analysis of more realistic conditions that might be encountered in the core. A transient suite of codes has been modified to include micro-scale models that determine the TRISO layer temperatures and internal gas pressures. This allows the feedback of parameters back to the engineering and meso-scale calculations. In addition, detailed conditions inside the fuel particle can now be used in the thermo-mechanical calculation for all regions in the core during the transient. This leads to the determination of the expected failure fraction of particles in the various regions of the core for a specific transient event. The precise location and inventory of material released

can then be used into a radioactive inventory transport model to finally calculate the predicted dose at the fence of the facility.

II. CALCULATION METHODS

II.A. General Coupled System

The Thermal TRISO (THETRIS) [1] fuel model included in this study is integrated in the coupled CYNOD [2] -THERMIX-KONVEK [3] suite of codes. Figure 1 shows a schematic of the coupling arrangement. The CYNOD neutronic solver initiates the power calculation and controls the time step. The volumetric heat generation rate is passed to THERMIX-KONVEK where the solid and fluid temperature fields are determined for the next time interval. The new bulk graphite temperature, $BC(t^{n+1})$, and the neutronic volumetric heat generation rate are subsequently used in THETRIS to resolve the fuel temperature in the kernels. This iterative scheme is performed at each time step until all fields meet their convergence criteria.

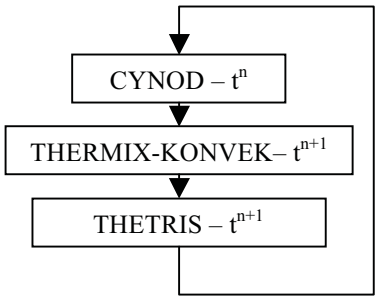

Figure 1. Coupling between the Neutronic and Thermal-Fluids codes.

II.A. Micro-Scale calculations

THETRIS solves the one-dimensional (1-D) Partial Differential Equation (PDE) system for the spatial domain $0 \le r \le r_s$ and temporal domain $t \ge 0$:

$$\nabla\cdot\left(k(r,t)\nabla T(r,t)\right)+q'''(r,t)=\frac{\partial\left(\rho(r,t)C_p(r,t)T(r,t)\right)}{\partial t} \quad \text{(eq 1)}$$
$$T(r_s,t)=T_g(t)$$
$$\left.\frac{\partial T(r,t)}{\partial r}\right|_{r=0}=0$$
$$T(r,0)=T_{SS}(r)$$

The thermo-physical properties k, r, and C_p are the thermal conductivity, density, and specific heat capacity, respectively. The exterior boundary condition is a fixed temperature at the boundary. The initial condition is the temperature field from a steady state calculation or a temperature field from a restart file.

The problem is simplified by assuming that the thermo-physical properties do not vary significantly between time steps, thus yielding the following:

$$\nabla\cdot\left(k(r)\nabla T(r,t)\right)+q'''(r,t)=\rho(r)C_p(r)\frac{\partial T(r,t)}{\partial t} \quad \text{(eq 2)}$$

for $0 \le r \le r_s$ for $t \ge 0$

Employing a theta time differencing scheme, using Fourier's law as the closure model, and forcing the continuity of the heat flux at the interfaces yields a three-point formulation for the average cell temperatures:

$$\theta\left(a_{i+1}\tilde{T}_{i+1}^{n+1}+a_i\tilde{T}_i^{n+1}+a_{i-1}\tilde{T}_{i-1}^{n+1}\right)=\left((1-\theta)q_i'''^{n}+\theta q_i'''^{n+1}\right)V_i$$
$$+(1-\theta)\left(b_{i+1}\tilde{T}_{i+1}^{n}+b_i\tilde{T}_i^{n}+b_{i-1}\tilde{T}_{i-1}^{n}\right) \quad \text{(eq 3)}$$

Since the final matrix is positive, definite, tri-diagonal, and symmetric, the direct inversion of the two-banded system of equations yields the final solution.

II.B. The THETRIS multi-pebble model

The original version of THETRIS did not contain a multi-pebble model. The coupling with CYNOD was performed by scaling the power density in the calculation cell to a power density for the TRISO kernel. This approach assumed that the power was equally distributed among all particle types:

$$q'''_{\text{ker}}=q'''_{neut}\frac{V_{peb}}{\psi N_T V_{\text{ker}}} \quad \text{(eq 4)}$$

where

q'''_{ker} = power density in a kernel
q'''_{neut} = power density from CYNOD calculation
$V_{peb/\text{ker}}$ = pebble/kernel volume
ψ = pebble packing fraction
N_T = number of TRISOs per pebble

In a more realistic reactor simulation each calculation cell may contain a variety of pebbles with different burnups and burnup histories that are crucial in the determination of the internal temperatures and pressures. The new THETRIS model takes into account various pebble types within one calculation cell.

In a system with random pebble recirculation, the number of pebbles of each type can be assumed equal $N_1=N_2=N_3\ldots=N$. This is a reasonable assumption since the total pebble recirculation for

each pebble type is the same. The total number of pebbles in a region with I pebble types is $N_p = IN$.

The average power density for all pebbles and the power density for the ith pebble type are related by an arithmetic average, assuming that the pebble and kernel volumes remain the same for all types,

$$q'''_{\text{ker}} = \frac{\sum_{i=1}^{I} q'''_{i,\text{ker}}}{I} \qquad \text{(eq 5)}$$

where

$q'''_{i,\text{ker}}$ = power density for the ith kernel type

I = number of pebble types in the cell

Results from the steady state code PEBBED [4] are used in the determination of the power density that is distributed to each kernel type. In PEBBED, the power for each pebble type is calculated as a function of core position during the recirculation calculations. The approach presented herein assumes that the distribution of power among the various pebble types during the transient remains the same as in the steady state core. From the PEBBED results, a power factor for each pebble type is computed with

$$P_{f,i} = \frac{\dot{q}_i}{\langle \dot{q}_i \rangle} = \frac{I\dot{q}_i}{\sum_{i=1}^{I} \dot{q}_i} \qquad \text{(eq 6)}$$

where

$\dot{q}_i$ = power in the pebbles of the ith type

$\langle \dot{q}_i \rangle$ = average power in the pebbles of the ith type

$P_{f,i}$ = power factor for pebbles of the ith type

This power factor also relates the power densities in the various pebble types

$$P_{f,i} = \frac{Iq'''_{i,\text{ker}}}{\sum_{i=1}^{I} q'''_{i,\text{ker}}} \qquad \text{(eq 7)}$$

Combining eq. 5 and eq. 7 leads to the simplified equation

$$q'''_{i,\text{ker}} = q'''_{\text{ker}} P_{f,i} \qquad \text{(eq 8)}$$

Finally, the substitution of eq. 8 into eq. 4 provides the mechanism to relate the power density from the neutronics calculation to that of each kernel type in the region

$$q'''_{i,\text{ker}} = P_{f,i} q'''_{neut} \frac{V_{peb}}{\psi N_T V_{\text{ker}}} \qquad \text{(eq 9)}$$

After the determination of the temperature fields for each pebble type the average kernel temperature must be computed to interpolate the cross sections:

$$T_f = \frac{\sum_{i=1}^{I} T_{f,i}}{I} \qquad \text{(eq 10)}$$

II.C. Fast Transient Correction

The power sent from CYNOD to THERMIX is assumed to be homogeneously distributed in the fuel region of the pebble. This can produce, in some instances, the incorrect boundary condition for the micro-scale code THETRIS, because all of the energy from the neutronics solution is deposited in the homogenized fuel region. This effect is not important during slow and moderately-slow transients, but it could be more significant during faster transients or when the kernel is more isolated from its surroundings, i.e. gap formation [1].

Physically, the heat generation due to energy deposition mostly takes place inside the fuel kernels. Integrating eq. 1 over the spatial domain leads to the time dependent balance equation for a coated particle model

$$\int_V \rho\,(r) C_p(r) \frac{\partial T(r,t)}{\partial t} dV = \int_V q'''_{i,T}(r) dV - \int_V \nabla \cdot \vec{q}_{i,T}(r) dV \qquad \text{(eq 11)}$$

where

$q'''_{i,T}$ = power density in a CP of the ith pebble type

$\vec{q}_{i,T}$ = heat flux in a CP of the ith pebble type

The last term on the right hand side represents the boundary term where heat transfer takes place with the surrounding material. These coated particles, which are distributed within the fuel region of the pebble, are the heat sources for the solid in the THERMIX code. The heat transfer through the boundary of the coated particles becomes the volumetric heat generation term for the specific pebble type

$$q'''_i = \frac{N_T}{V_{peb}} \int_V \nabla \cdot \vec{q}_{i,T}(r) dV \qquad \text{(eq 12)}$$

Using Gauss' divergence theorem the volume integral can be equated to the heat transferred through the surfaces

$$q_i''' = \frac{N_T}{V_{peb}} \int_{\partial S} \vec{q}_{i,T}(r) \cdot d\vec{A} = \frac{N_T}{V_{peb}} A_s \vec{q}_{i,T}(r_s) \qquad \text{(eq 13)}$$

where

A_s = area of the surface

r_s = position of the surface

The corrected power density that must be passed to THERMIX is obtained by multiplying eq. 13 by the ratio of the pebble to calculation cell volume, thus obtaining

$$q'''_{THERMIX} = \frac{\psi N_T}{V_{peb}} \frac{\sum_{i=1}^{I} \vec{q}_{i,T}(r_s) A_s}{I}. \qquad \text{(eq 14)}$$

The only piece missing is the surface flux for the i^{th} TRISO particle, which can be calculated from the balance equation (eq. 11) by rearranging the terms and using Gauss' divergence theorem on the heat flux term

$$\vec{q}_{i,T}(r_s) A_s = \int_V \left[q'''_{i,T}(r) - \rho\,(r) C_p(r) \frac{\partial T(r,t)}{\partial t} \right] dV \qquad \text{(eq 15)}$$

This formulation modifies the volumetric heat generation that the homogeneous model uses in order to account for the energy that is deposited internally in the TRISO particles.

An schematic of the calculation flow is shown in Figure 2. The volumetric heat generation rate from the neutronic calculation and bulk graphite temperature from the current time step, $BC(t^n)$, are used in an initial THETRIS calculation to determine an initial coated particle temperature field. A new volumetric heat generation rate for the homogeneous model is computed with eq. 14. THERMIX-KONVEK then calculates the solid and fluid temperature fields, respectively, at the next time interval with this corrected volumetric heat generation rate. The new bulk graphite temperature, $BC(t^{n+1})$, and the neutronic volumetric heat generation rate are subsequently used in THETRIS to resolve the fuel temperature in the kernels. This iterative scheme is performed at each time step until all fields meet their convergence criteria.

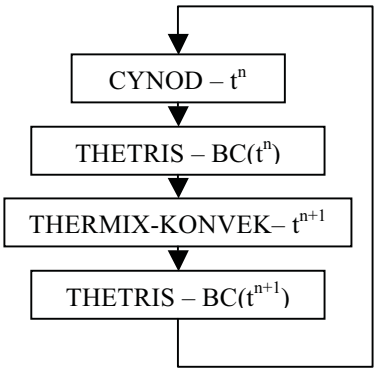

Figure 2. Coupling between the Neutronic and Thermal-Fluids codes with power correction.

II.D. Gas Release Models

Several simplified gas release models are included in the THETRIS code. The initial focus of the gas models was to determine the gap thermal conductivity during gap formation to better approximate the temperature feedback [1]. Since the gas pressure and temperature evolutions are computed during the transient it seems natural to feed this data into the stress analysis models in PASTA [5,6].

The calculation of the internal gas pressure for each particular species uses the Redlich-Kwong equation of state:

$$P_i = \frac{RT}{V_i - b_i} - \frac{a_i}{V_i(V_i + b_i)T^{1/2}} \qquad \text{(eq 16)}$$

where

P_i= partial pressure for the i^{th} species
R= 8.314472 $cm^3 \cdot MPa \cdot K^{-1} \cdot mol^{-1}$
T = gas temperature ,K
a,b = parameters for the i^{th} gas species
$V_i = V_{gas}/n_i$ = i^{th} species molar volume
V_{gas} = gas volume available
n_i = number of moles for the i^{th} species

The number of moles of the gas species (Xe, Kr, or CO) is the oxide fuel kernel is calculated with:

$$M = M_k \cdot FIMA \{FY_{Kr/Xe}, O/f\} \qquad \text{(eq 17)}$$

Where

M_k = moles of metal atoms in the kernel

FIMA= fraction of initial heavy metal atoms fissioned

$FY_{Kr/Xe}$= fission yield of krypton or xenon,

O/f = Oxygen released at the end of irradiation (atoms per fission)

The fraction of fission gases that are released into the void region is approximated with a Booth release model. The model assumes that initially there are no gases present, the generation of fission products is homogeneous, and under the steady state and transient conditions are [7]:

$$F_{SS} = 1.0 - \frac{6}{D't}\sum_{n=1}^{\infty}\frac{1-e^{-n^2\pi^2 D't}}{n^4\pi^4} \qquad \text{(eq 18)}$$

$$F_{TR} = 1.0 - 6\sum_{n=1}^{\infty}\frac{e^{-n^2\pi^2 D'\Delta t}}{n^2\pi^2} \qquad \text{(eq 19)}$$

Where

t = irradiation time in seconds,
Δt = time step,
D'= effective diffusivity

For Xe and Kr in UO_2 the effective diffusivity is given by [8]:

$$D' = 5.0E - 3e^{-Q_o/RT} \qquad \text{(eq 20)}$$

where
Q_o= 155.4 kJ/mol
T = irradiation temperature [K].

The number of oxygen gas atoms released per fission at steady state is calculated with [9,10]:

$$\left(O/f\right)_{SS} = 8.32x10^{-11}t^2\exp\left(-\frac{162.7\,kJ/mol}{RT}\right) \qquad \text{(eq 21)}$$

where
T = time-averaged particle surface temperature during irradiation. (K)

The same equation during heating is modified to the equation proposed by Liang [11]:

$$\left(O/f\right)_{TR} = \left(O/f\right)_{SS} 10^{-4040\left(\frac{1}{T_h}-\frac{1}{T_i+75}\right)} \qquad \text{(eq 22)}$$

Where T_h = heating temperature
T_i = irradiation temperature
t= irradiation time in days

The data for the thermal conductivity of the gases and the calculation methodology has been obtained from RELAP5-3D© [12]. The individual gas conductivities are calculated with

$$k = AT^B \qquad \text{(eq 23)}$$

where
T= gas temperature in K
A and B = gas parameters for the species

II.E. Stress Models

The PASTA code [5, 6] describes the mechanical behavior of TRISO particles during irradiation and aims at calculating the coating stresses and the corresponding failure probabilities. PASTA embodies a one-dimensional analytical and multi-layer model that takes into account the visco-elastic behavior of the coating layers and the surrounding graphite during irradiation. The main source of stress in all layers is due to the pressure build-up from the gaseous fission products in the buffer layer resulting in a radial stress on the IPyC.

Moreover, the Pyrocarbon (IPyC and OPyC) layers exhibit radiation-induced dimensional changes and creep (in the radial and tangential directions). Finally, the model allows thermal expansion of all layers. PASTA solves the general stress strain equations in spherical geometry, which include the aforementioned effects.

The mechanical failure probability of the coated particle is determined from the magnitude of the (tensile) stress in the SiC layer, which is the main load bearer, according to a Weibull distribution [13].

The PyC coating layers exhibit a dimensional change under irradiation in a fast neutron flux. The dimensional change change as a function of the fast neutron fluence (E >0.18 MeV) is fitted for several temperatures and Bacon Anisotropy Factors (BAFs) [14]. Table 1 shows an overview of the data used in PASTA for the mechanical properties.

I/OPyC Material property	Value
Young's modulus of elasticity [MPa]	3.96×10^4
Poisson's ratio [-]	0.33
Poisson's ratio of creep [-]	0.4
Creep coefficient $[10^{25}(MPa.m^{-2})^{-1}]$	2.0×10^{-4}
Dimensional change rate $[10^{25}(MPa.m^{-2})^{-1}]$	Dose dependent [14]
Thermal expansion coefficient $[K^{-1}]$	Temperature dependent [13]
Bacon Anisotropy Factor	1.0
SiC Material property	
Young's modulus of elasticity [MPa]	4.0×10^5
Poisson's ratio [-]	0.13
Thermal expansion coefficient $[K^{-1}]$	Temperature dependent [13]

Table 1. Material property data used in PASTA analysis.

Recently, the PASTA code was coupled to the PEBBED code [4] for neutronic, thermal-hydraulic and depletion analysis of pebble-bed cores. This coupled code system [15] allows for the determination of the coated particle performance as a function of the local and time dependent core parameters (temperature, kernel power, fast fluence level, burn-up level, core residence time and fission product (Xe, Kr) concentration). This allows for determination of the stress effects caused by the power and temperature peaking that are typically found in an HTR core design.

The variation in the thicknesses of the coating layers that can be found in a typical batch of particles is treated by a statistical method. Furthermore, stresses can be evaluated for various transient cases. In this case the history of the input parameters for the normal operation, generated with the PEBBED code, are augmented with input from the transient analysis [15]. In the transient analysis of this paper the input data for PASTA is provided by the CYNOD-THETRIS-THERMIX codes.

III. ANALYSIS MODEL

The model used in this analysis is the same used in the PBMR-400 benchmark exercise [16], which contains 6 different pebble types. Figure 3 shows the thermal-fluids material regions.

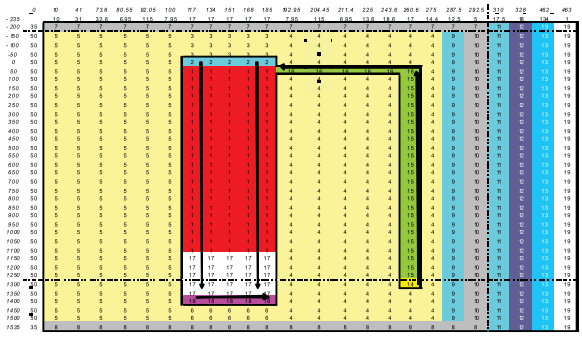

Figure 3. Thermal-Fluids Layout of PBMR Core

The helium coolant path is bordered by the solid lines superposed on the model. The helium enters the core in the side reflector's lower inlet plenum (region 14). The gas flows upwards through the riser channels (region 15) into the upper inlet plenum (region 16). The gas then flows down the pebble bed core (region 1) and through a set of slits in the bottom reflector (region 17), into the outlet plenum (region 18). From the outlet plenum it enters the power conversion unit. Areas of stagnant helium include the area between the side reflector (region 4) and the barrel (region 10), and between the barrel and the Reactor Pressure Vessel (RPV) (region 12). Stagnant air in modeled between the RPV and Reactor Cavity Cooling System (RCCS) (region 19). The only heat transfer mechanisms modeled in this regions are conduction and radiation heat transfer. No regions of bypass flow are included in the model. The axial portion of the thermal-fluids model uses an adiabatic boundary condition, whereas the radial portion uses an isothermal boundary condition.

The neutronic definition is a subset of the thermal-fluids domain and extends only to the core barrel. The actual transient used in this analysis is the Total Control Rod Ejection (TCRE), since it provides an extreme case to test the microscopic codes.

IV. RESULTS

Figure 4 shows the average fuel temperature and relative core power during the first 10 seconds of simulation. The relative power of the core peaks at 41 times nominal while the average fuel temperature in the core nears 1200 ^{o}C.

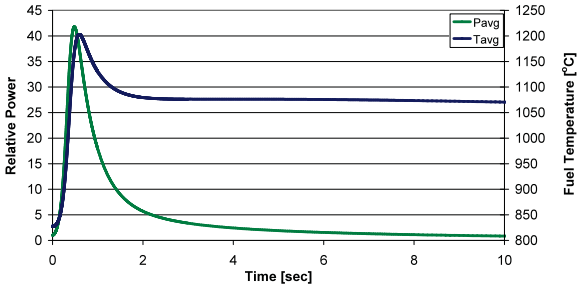

Figure 4. Average fuel temperature and relative core power in the PBMR-400 during a TCRE.

Results from the fast transient correction implemented in the code system are included in Figure 5. The three terms from the balance equation applicable to all TRISO particles in the core are shown.

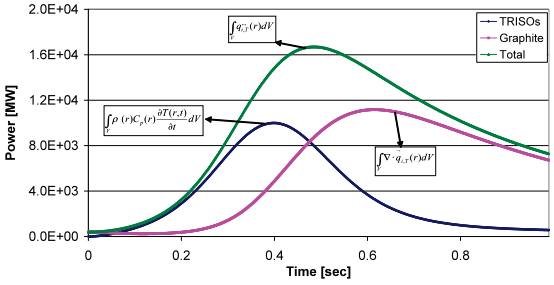

Figure 5. Rate of heat transfer from the neutronics into the TRISOs and core graphite in the 1st second of transient.

For this specific transient, the rate of change of the internal energy of the TRISOs dominates the first part of the transient, reaching its maximum at 0.4 seconds. The rate of energy flow out of the TRISO particles and into the graphite is delayed and

reaches its peak at 0.6 seconds. This plot shows the shift from heating the TRISO particles to heating the surrounding graphite.

Figure 6 and 7 include the average and maximum fuel temperatures, respectively, for each pebble type in the core. The highest core-averaged fuel temperature for each fuel type ranges from 1100 to over 1250 °C, which is consistent with the previous value of 1200 °C for the core average. The maximum fuel temperature occurs in the type 1 fuel, since it is the fresh batch. This maximum is 2046 °C, whereas Type 6, which is fuel with considerable burnup, reaches a maximum temperature of 1553 °C.

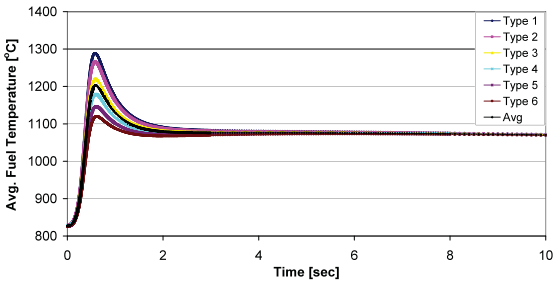

Figure 6. Average fuel temperature for each pebble type in the PBMR-400 during a TCRE.

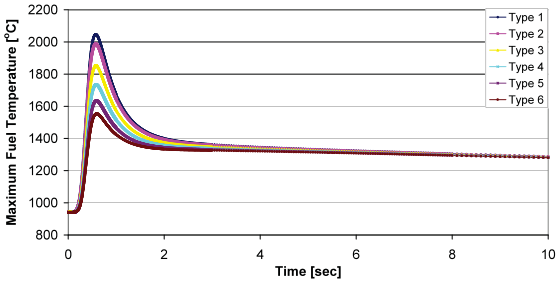

Figure 7. Maximum fuel temperature for each pebble type.

The two parameters used in the PASTA stress calculations are the average temperature in the three (IPyC, SiC, OPyC) layers and the internal gas pressure. Figure 8 shows the average of these layers for the first ten seconds of simulation.

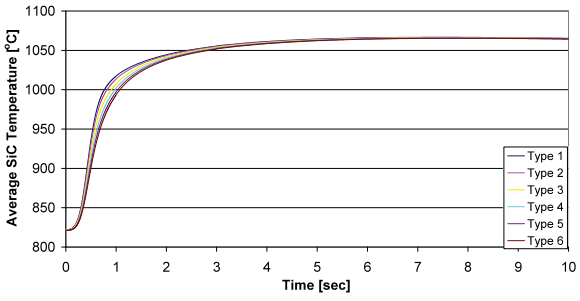

Figure 8. Average (IPyC-SiC-OPyC) temperature for each pebble type.

The progression of the TRISO internal gas pressure distribution in the core is shown in Figure 10 for pebble type 6. In the steady state condition the pressure peak is located at the bottom of the core, where the highest burnups and temperatures occur, as indicated by Figure 10(a). During the transient, the control rods are ejected from the top of the core, thus inducing a strong power and temperature peak in that region. Figure 10(b) indicates that this maximum temperature is most pronounced near the central reflector. The high fuel temperatures enhance the diffusion of fission gasses and CO into the void regions of the porous carbon layer, thus increasing the internal pressure. The peak pressure occurs 4.7 seconds into the transient. After 40 seconds, Figure 10(c), the gas pressure is decreasing in the peak power region and increases in other regions as the core temperature distribution starts to equilibrate.

Figure 9 includes the stress history during the recirculation and transient condition. The discontinuities correspond to recirculation steps during the life of the pebble. As the recirculation progresses the SiC layer is maintained under compressive stress, while the PyC layers remain in tensile stress. The transient forces a change of stress regime from compressive to tensile for the SiC layer, but not of significant magnitude.

Detailed stress distributions at three points during the transient for the type 6 pebbles are shown in Figure 11. The stress distribution follows that of the temperature and pressure in the TRISO particles. A maximum internal TRISO pressure of 26 MPa occurs for a type 6 pebble circulated near the central reflector. Figure 9 shows that the SiC tangential stress climbs to 20.4 MPa. The results from PASTA suggest that this will cause a local particle failure fraction of 5.5 x 10^{-7} and an average failure fraction for pebble Type 6 of 9.4 x 10^{-9}.

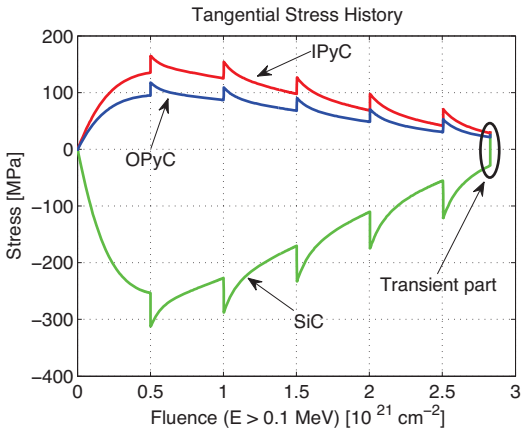

Figure 9. Tangential stress history for a pebble near the center reflector.

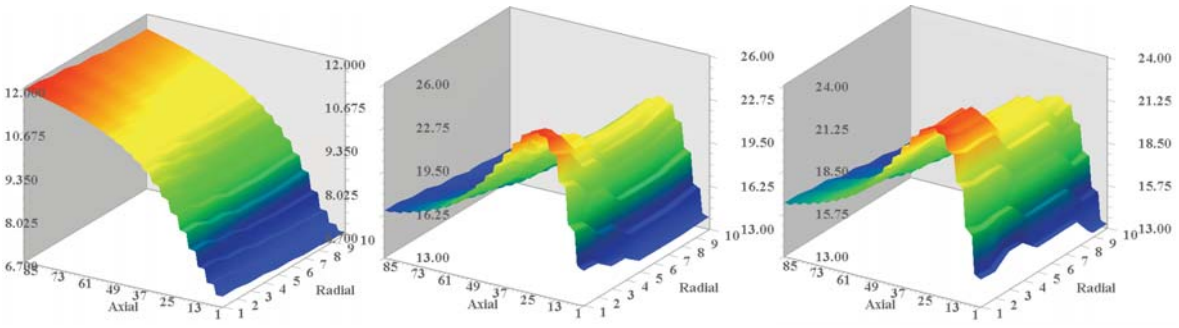

(a) (b) (c)

Figure 10. Internal TRISO pressure for pebbles of type 6 in the core at the beginning of the transient (t = 0 s) (a), at the time point of the peak pressure (t =4.7 s) (b) and at the end of the transient (t = 40 s) (c).

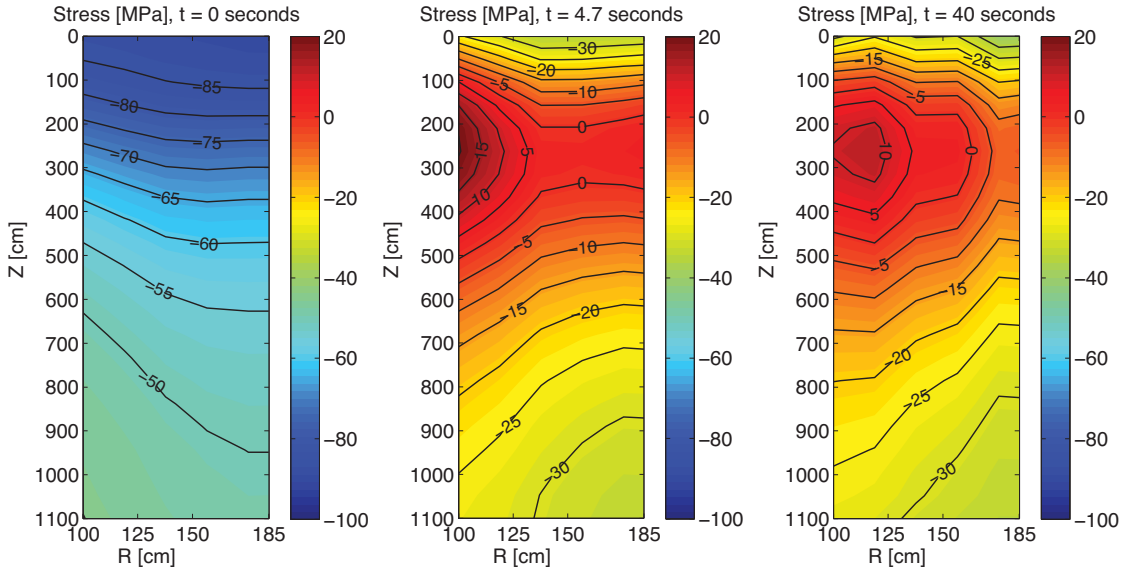

(a) (b) (c)

Figure 11. The tangential stress of the SiC layer as a function of the pebble location in the core at the beginning of the transient (t = 0 s) (a), at the time point of the peak stress (t =4.7 s) (b) and at the end of the transient (t = 40 s) (c).

V. CONCLUSION

This paper includes some of the capabilities for the performance of transient and thermo-mechanical analysis at the INL for pebble bed reactors. The results show that a TCRE event does not pose a significant challenge to the integrity of the TRISO particles. The maximum internal gas pressure attained during the transient is 26 MPa, while the corresponding tangential stress is 20 MPa. Magnitudes in the hundreds of MPa are required to induce large numbers of failures in this type of fuel. The average failure fraction in the core for the fuel with the highest burnup is in the order of 1x 10^{-8}.

The new features included in the THETRIS module allow the calculation of the various layer temperatures and internal gas pressures. These parameters are calculated for all pebble types in each region of the core and are subsequently analyzed in PASTA to provide a more realistic simulation of the local core conditions.

ACKNOWLEDGEMENTS

Work supported by the U.S. Department of Energy, Office of Nuclear Energy, under DOE Idaho Operations Office Contract DE-AC07-05ID14517.

REFERENCES

1. Ortensi, J., Ougouag, A.M., Improved Prediction of the Temperature Feedback in TRISO-Fueled Reactors, INL/EXT-09-16494, August 2009.

2. Hiruta, H., et al., 2008, CYNOD: a Neutronics Code for Pebble Bed Modular Reactor Coupled Transient Analysis, HTR2008, September 28–October 1, 2008, 4th International Topical Meeting on High Temperature Reactor Technology.

3. Teuchert, E., et al., 1994, V.S.O.P. ('94) Computer Code System for Reactor Physics and Fuel Cycle Simulation - Input Manual and Comments, April 1994.

4. W. K. Terry, H. D. Gougar, A. M. Ougouag. Direct Deterministic Method for Neutronics Analysis and Computation of Asymptotic Burnup Distribution in a Recirculating Pebble-Bed Reactor. Annals of Nuclear Energy, 29, p. 1345–1364, 2002.

5. B. Boer, A. M. Ougouag, J. L. Kloosterman, G. K. Miller. Stress analysis of coated particle fuel in graphite of High-Temperature Reactors. Nuclear Technology, 162, p. 276–292, 2008.

6. J. Jonnet, J. L. Kloosterman, B. Boer. Development of a stress analysis code for TRISO particles in HTRs. In Proceedings of the International Conference on the Physics of Reactors (PHYSOR-2008), Nuclear Power: A Sustainable Resource. Switzerland, 2008.

7. Nabielek, H., Myers B.F, Fission Product Retention HTR Fuel, Gas Cooled Reactors Today, BNES, London, 1982.

8. Nabielek H., Verforndern K., Werner H., "Can we predict coated particle failure?" Technical Meeting on Current Status and Future Prospects of Gas Cooled Reactor Fuels, IAEA, Vienna, 7-9 June 2004.

9. Nabielek H., Partikeln und Brennelemente für den HTR, KFA-HTA Report, 1991.

10. Proksch E., Strigl A., Nabielek H., Production of Carbon Monoxide During Burn-up of UO_2 Kerneled HTR Fuel Particles, J. Nuc. Mat. 107 (1982) pp. 280.

11. Liang, T.X., Zhao H.S., Tang C.H., Verfondern K., Irradiation performance and modeling of HTR-10 coated fuel particles, nucl. eng. des. 236 (2006) pp. 1922.

12. RELAP5-3D© Manuals, Volume 4: Models and Correlations, INEEL-EXT-98-00834-V1,06/2005.

13. L. L. Snead, T. Nozawa, Y. Katoh, T.-S. Byun, S. Kondo, D. Petti. Handbook of SiC properties for fuel performance modeling. Journal of Nuclear Materials, 371, p. 329–377, 2007.

14. F. Ho. Material Models of Pyrocarbon and Pyrolytic Silicon Carbide. Technical Report CEGA-002820, CEGA Corporation, San Diego, CA, 1993.

15. B. Boer, A. M. Ougouag. Stress Analysis of Coated Particle Fuel in the Deep-Burn Pebble Bed Reactor Design In Proceedings of the PHYSOR 2010 - Advances in Reactor Physics to Power the Nuclear Renaissance. American Nuclear Society, Pittsburgh, USA, May 2010.

16. OECD/NEA/NSC PBMR Coupled Neutronic/Thermal Hydraulics Transient Benchmark: The PBMR-400 Core Design, Draft 07 (2007).